Nitric Oxide Regulates the *Ralstonia solanacearum* Type 3 Secretion System

Connor G. Hendrich[1], Alicia N. Truchon[1], Beth L. Dalsing[1,2], and Caitilyn Allen[1*]

[1] Department of Plant Pathology, University of Wisconsin – Madison, Madison, Wisconsin, USA

[2] Present address: Syngenta, Durham, NC

[*] Correspondence: callen@wisc.edu (Caitilyn Allen)

Keywords: *Ralstonia solanacearum*, Type III Secretion, nitric oxide, bacterial wilt, vascular wilt, tomato

Abstract

Ralstonia solancearum causes bacterial wilt disease on diverse plant hosts. *R. solanacearum* cells enter a host from soil or infested water through the roots, then multiply and spread in the water-transporting xylem vessels. Despite the low nutrient content of xylem sap, *R. solanacearum* grows extremely well inside the host, using denitrification to respire in this hypoxic environment. *R. solanacearum* growth *in planta* also depends on the successful deployment of protein effectors into host cells using a Type III Secretion System (T3SS). The T3SS is absolutely required for *R. solanacearum* virulence, but it is metabolically costly and can trigger host defenses. Thus, the pathogen's success depends on optimized regulation of the T3SS. We found that a byproduct of denitrification, the toxic free-radical nitric oxide (NO), positively regulates the *R. solanacearum* T3SS both *in vitro* and *in planta*. Using chemical treatments and *R. solanacearum* mutants with altered NO levels, we show that the expression of a key T3SS regulator is induced by NO in culture. Analyzing the transcriptome of *R. solanacearum* responding to varying levels of NO both in culture and *in planta* revealed that the T3SS and effectors were broadly upregulated with increasing levels of NO. This regulation was specific to the T3SS and was not shared by other stressors. Our results suggest that *R. solanacearum* experiences an NO-rich environment in the plant host and may use this NO as a signal to activate T3SS during infection.

Introduction

Ralstonia solancearum (*Rs*) is a Gram-negative soil-borne betaproteobacterium that causes bacterial wilt disease on a wide range of plant hosts, including important crops like tomato, potato, and banana (Elphinstone, 2005). The bacteria survive in and are spread through infected soil and water, infecting host roots through wounds and natural openings (Vasse *et al.*, 1994). Once inside, *R. solanacearum* cells move to the xylem, where they can grow and spread throughout the plant. Although this bacterium is slow growing and sensitive to stress when grown *in vitro*, in plant xylem vessels *R. solanacearum* is a formidable force. *R. solanacearum* quickly grows to high cell densities in xylem even

55 though this habitat is low in oxygen and nutrients, and accessible to host defenses (Genin and Denny,
56 2012). As it grows, *R. solanacearum* produces an arsenal of virulence factors, including highly mucoid
57 extracellular polymeric substances (EPS), a consortium of cell wall degrading enzymes, and dozens of
58 protein effectors that are injected into host cells via the Type III Secretion System (T3SS) (Genin and
59 Denny, 2012). Water transport in infected plants is eventually blocked by a combination of host-produced
60 gels and tyloses, degradation of vessel walls, EPS, and the sheer mass of bacterial cells. Without
61 sufficient water, plants wilt and die while *R. solanacearum* cells escape back into the soil, where they can
62 find another host (Swanson *et al.*, 2007).

63 The lethality of bacterial wilt disease combined with its wide host range and a lack of effective
64 treatments make *R. solanacearum* an important agricultural problem around the world (Elphinstone,
65 2005; Yuliar *et al.*, 2015). Successful disease management depends on understanding *R. solanacearum*
66 biology, but the pathogen behaves very differently in culture than it does in its natural environment
67 (Jacobs *et al.*, 2012). In particular, the T3SS, which is absolutely essential for virulence and subject to a
68 complex regulatory cascade, is affected by the plant environment in ways that remain poorly understood
69 (Poueymiro and Genin, 2009). The PhcA quorum sensing system upregulates T3 secretion in culture, but
70 not *in planta* (Génin *et al.*, 2005; Jacobs *et al.*, 2012; Khokhani *et al.*, 2017; Monteiro, Genin, *et al.*, 2012).
71 An unidentified 'diffusible factor' increases T3SS expression *in planta* via the HrpG global regulator
72 (Genin and Denny, 2012).

73 We have discovered that the diffusible free radical nitric oxide (NO) plays a role in *R.*
74 *solanacearum* life inside plants. Xylem sap is rich in nitrate, which *R. solanacearum* uses as an alternate
75 electron acceptor to respire in the hypoxic xylem environment (Dalsing *et al.*, 2015). The *R.*
76 *solanacearum* strain GMI1000 reduces nitrate completely to dinitrogen gas by means of denitrifying
77 respiration. The genes required for this process are highly expressed during infection (Jacobs *et al.*,
78 2012; Khokhani *et al.*, 2017). However, denitrifying respiration produces NO as an intermediate. In large
79 quantities, NO is toxic and strongly inhibits *R. solanacearum* growth. The pathogen manages this threat
80 by detoxifying NO with the nitric oxide reductase NorB and the flavohemoglobin HmpX, which are both
81 highly expressed *in planta* and required for full virulence (Dalsing *et al.*, 2015; Jacobs *et al.*, 2012). Plants

82 use NO extensively for both signaling and defense, and can produce NO through multiple different
83 pathways (Delledonne *et al.*, 1998; Leitner *et al.*, 2009; Scheler *et al.*, 2013; Simontacchi *et al.*, 2015;
84 Wilson *et al.*, 2008). Thus, *R. solanacearum* likely encounters NO during plant pathogenesis.
85 In this study, we identify a link between NO and regulation of the *R. solanacearum* T3SS. We first
86 show that T3SS gene expression increases when *R. solanacearum* is actively denitrifying. We then show
87 that this effect depends specifically on the presence of NO. Based on these results, we conducted a
88 transcriptomics experiment to determine the effects of NO on *R. solanacearum* gene expression in culture
89 and *in planta* and show that levels of many transcripts, including 107 T3SS-related genes, are altered by
90 changes in NO levels.
91
92 **Results**
93 **Nitric oxide changes expression of the *R. solanacearum* T3SS**
94 Regulation of the T3SS in *R. solanacearum* is multi-layered and incompletely understood (Figure
95 1a). Because *R. solanacearum* actively denitrifies *in planta*, we wondered if this pathway or its products
96 affect T3SS expression during plant infection (Dalsing *et al.*, 2015; Jacobs *et al.*, 2012). To test this
97 hypothesis, we used an *R. solanacearum* reporter strain carrying a fusion of the *lux* operon to the
98 promoter of *hrpB*, which encodes a key T3SS regulator (Genin and Denny, 2012). Transcription of *hrpB*
99 increased >3-fold when the bacterium was denitrifying in culture (Figure 1b). We therefore further
100 explored how denitrification and NO specifically affect *hrpB* expression. We incubated a *hrpB::lux* cell
101 suspension with tomato seedlings for 24 hours with or without the NO scavenger cPTIO (Pfeiffer *et al.*,
102 1997). As expected, the presence of a host plant activated *hrpB* gene expression but adding cPTIO to the
103 mixture completely reversed this effect (Figure 1c). This indicated that the denitrifying respiration-
104 dependent increase in *hrpB* expression that we observed in culture is specifically triggered by NO.
105 Further, this result suggests that NO could be the unknown soluble signal that increases *hrp* regulon
106 expression *in planta*.

107

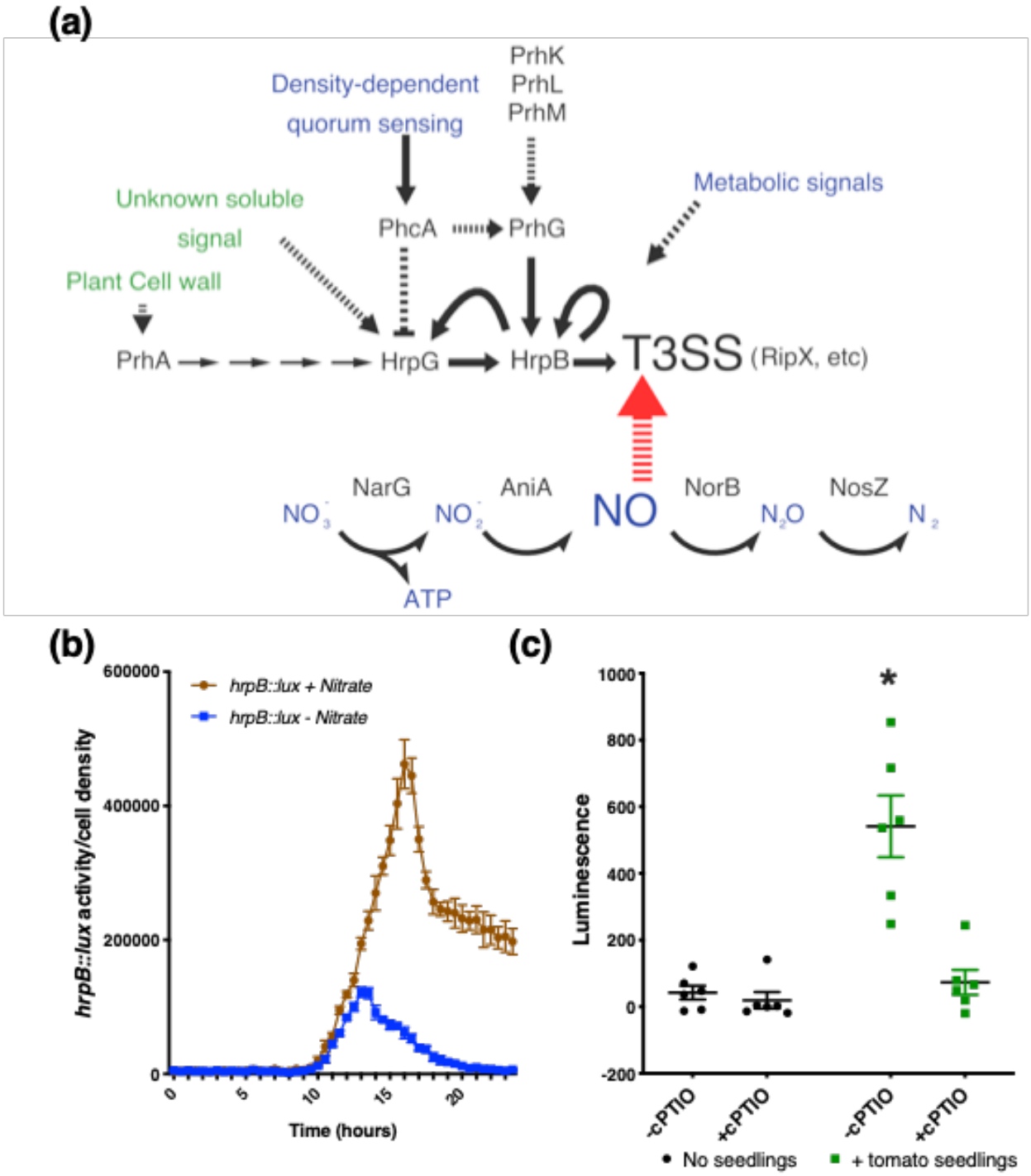

108

109 **Figure 1 Nitric oxide affects expression of the *R. solanacearum* T3SS. (a)** Summary of known T3SS

110 regulation in *R. solanacearum* strain GMI1000. Arrows indicate positive regulation, barred lines indicate

111 repression, dashed lines indicate an unknown or uncharacterized mechanism, green text indicates plant-

112 derived signals, and blue text indicates metabolites. T3SS genes, such as the T3 effector *ripX*, are
113 controlled by the transcriptional regulator HrpB. HrpB is transcriptionally activated by HrpG and PrhG,
114 which are themselves controlled by the quorum-sensing regulator PhcA, but only *in vitro*. PrhG activity
115 also depends on three uncharacterized proteins, PrhK, PrhL, and PrhM, through an unknown mechanism.
116 HrpG is activated by the contact-dependent plant cell wall sensor PrhA as well as by an unknown soluble
117 signal present during plant infection. **(b)** Expression of a bacterial luciferase transcriptional reporter of
118 HrpB. *R. solanacearum* strain GMI1000 *hrpB::lux* was grown in denitrification-inducing conditions with or
119 without 30 mM nitrate. Both culture density (OD_{600}) and luminescence were measured every 30 min, and
120 luminescence was normalized to culture density. Error bars represent standard error of the mean.
121 Cultures grown with nitrate had significantly increased *hrpB* expression (2-way ANOVA, P=0.0003). **(c)**
122 The NO scavenger cPTIO decreased T3SS activity in the presence of a host. Luminescence of *R.*
123 *solanacearum hrpB::lux* was measured after 24 h incubation in water with or without five day-old tomato
124 seedlings, and with or without 1 mM cPTIO, an NO-scavenger. Exposure to tomato seedlings induced
125 *hrpB::lux* expression (P=0.004, students T test). *R. solanacearum* cells exposed to both tomato seedlings
126 and cPTIO had luminescence indistinguishable from that of cells without tomato seedlings. Error bars
127 represent standard error of the mean.
128
129 **Denitrifying metabolism causes broad changes in *R. solanacearum* gene expression.**
130 To better understand the effects of NO on *Rs* biology, we sequenced the transcriptomes of *R.*
131 *solanacearum* cells grown with varying levels of NO both in culture and in infected tomato plants (Figure
132 2a). In culture, we grew the cells in 0.1% O_2 in a modified Van den Mooter medium (VDM), which
133 promotes denitrifying respiration (Dalsing *et al.*, 2015). We manipulated intracellular *R. solanacearum* NO
134 levels genetically by using mutants lacking either the NarG nitrate reductase (the *ΔnarG* mutant cannot
135 denitrify and does not produce NO), or the NorB nitric oxide reductase (the *ΔnorB* mutant accumulates
136 NO, see Supplementary Figure 1). Exogenous NO levels were manipulated by treating cells with CysNO,
137 a nitrosothiol NO donor. Because high NO levels are toxic to *R. solanacearum*, we controlled for general
138 stress responses by also profiling transcriptomes of cultures treated with H_2O_2, a non-NO source of

139 stress. After about 18 h, growth of the *ΔnorB* mutant was inhibited by accumulating NO, so we sampled
140 cultures 16 hpi, when *ΔnarG*, *ΔnorB*, and the wild-type strain were at similar densities (Supplementary
141 Figure 1). CysNO or H_2O_2 treatments were added 4 h before sampling, at the highest concentrations that
142 did not significantly alter culture growth (Supplementary Figure 2a). Total RNA was extracted from
143 bacteria *in planta* 3 days after tomato plants were inoculated with ~2000 CFU of *R. solanacearum*
144 through a cut petiole (Khokhani *et al.*, 2017). This method synchronized the infection process better than
145 root inoculation. Bacterial colonization in sampled tissue was standardized by extracting RNA only from
146 stems containing between $5x10^7$ and 10^9 CFU/g stem, as determined by dilution plating a ground stem
147 section (Supplementary Figure 2B). Each of the three biological replicates contained pooled RNA from 4
148 or 5 plants.

149

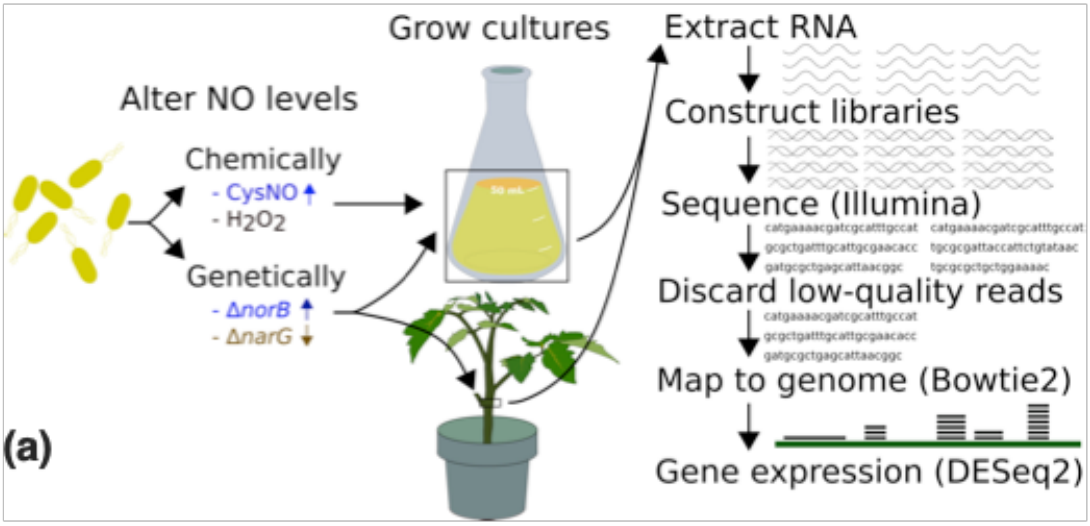

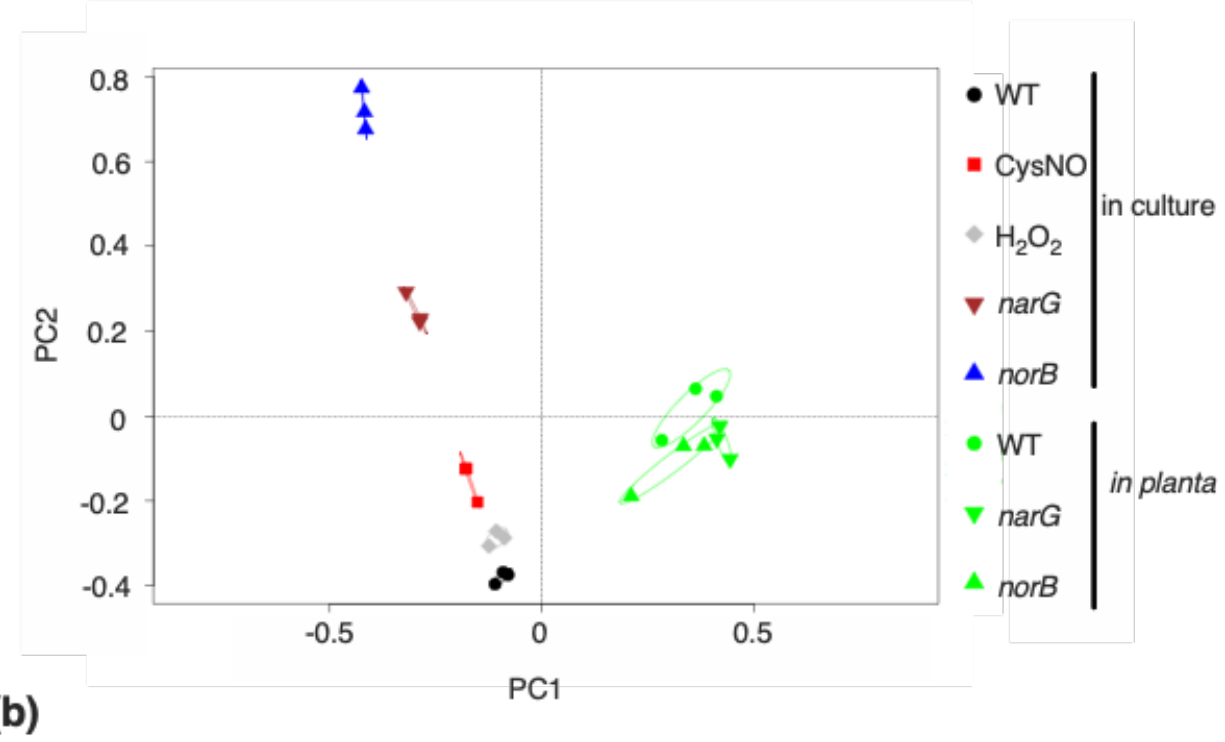

150

151 **Figure 2 Nitric oxide causes broad changes in *R. solanacearum* gene expression**. **(a)** Design of

152 RNA-seq experiment. We extracted RNA from *R. solanacearum* grown with altered NO levels from stems

153 of infected tomato plants (*in planta)* and from denitrifying VDM medium (in culture) and NO levels were

154 increased chemically by adding the NO donor CysNO to wild type (WT) and increased genetically by

155 using a NO-accumulating *Δ*norB mutant. The *ΔnarG* mutant has reduced levels of NO. H_2O_2 -treated WT
156 was included as a control for non-nitrosative general stress responses. **(b)** Whole-transcriptome datasets
157 were used for principal component analysis; plot created in R with the package Vegan (Oksanen, *et al.*,
158 2019). Each data point represents one biological replicate, with three replicates per condition. Ellipses
159 represent a 95% confidence interval for each condition (some ellipses are so small that they appear as
160 lines).
161
162 Around 97% of RNA-seq reads from *in vitro* samples mapped to the *R. solanacearum* genome
163 (Supplementary Figure 3A). Because tomato stem slices also included host RNA, only 9.2% of the *in*
164 *planta* RNA reads mapped to the *R. solanacearum* genome. However, the absolute number of bacterial
165 transcripts from the *in planta* samples still exceeded 10^6 reads per replicate. Principal component
166 analysis clustered the *in vitro* samples together based on treatment, and the *in planta* samples were even
167 more tightly clustered, reflecting less variation in gene expression than the culture samples (Figure 2b).
168 Genes were considered differentially expressed if they had an adjusted P-value <0.05. A full list of gene
169 expression values can be found in Supplementary Table 2.
170 We validated our transcriptomic results by using qRT-PCR to measure the expression of two
171 regulators of T3SS, *hrpB* and *hrpG*, and one well-expressed T3E, *ripX*. Expression levels of each of these
172 genes in the *ΔnarG* and *ΔnorB* mutants closely matched those obtained from RNA-seq analysis (Figure
173 3). As with *hrpB* expression, *hrpG* and *ripX* were both activated by NO, whether it was produced
174 endogenously or exogenously.

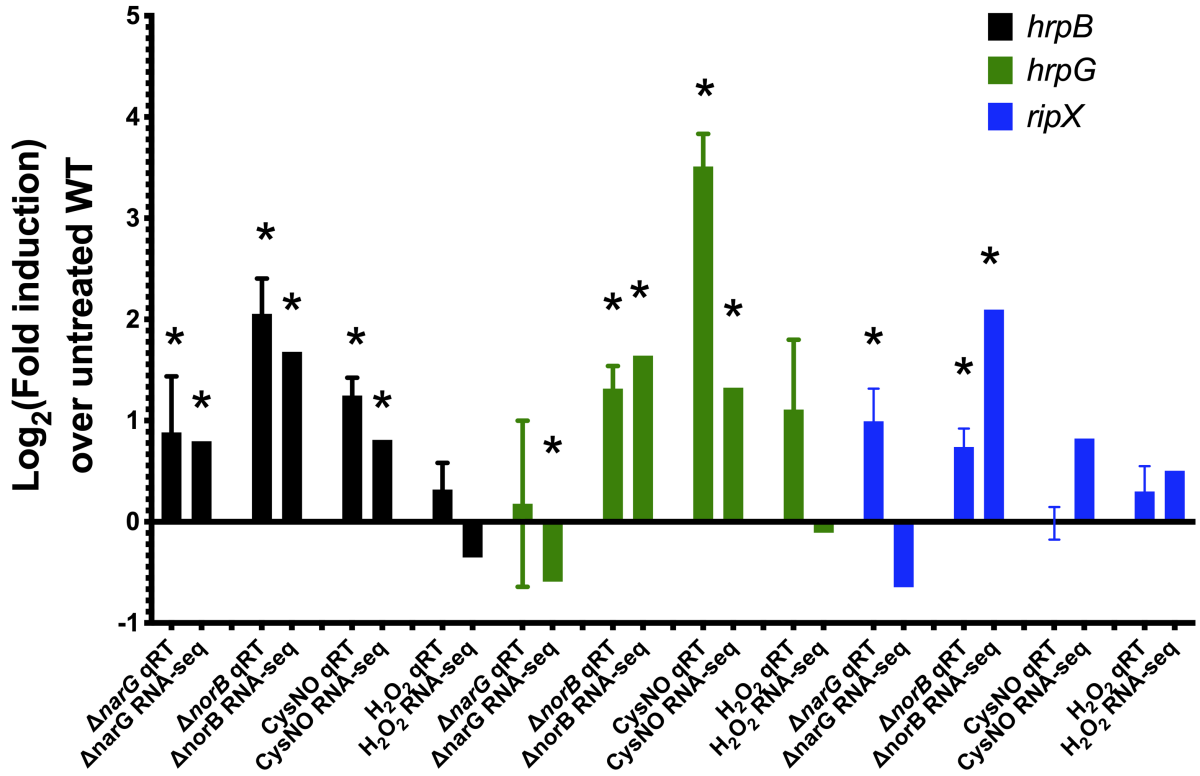

175

176 **Figure 3 Expression analysis of selected T3SS-related genes by qRT-PCR validated RNA-seq**
177 **results.** RNA was extracted from *R. solanacearum* cultured in VDM media at 0.1% oxygen for 16 hours
178 for both qRT-PCR and RNA-seq analysis. *R. solanacearum* samples were: wild type strain GMI1000 (WT,
179 untreated control reference), non-denitrifying low-NO mutant *(ΔnarG*) and NO-accumulating mutant
180 (*ΔnorB*), and WT treated for 4h with exogenous NO (CysNO). Gene expression levels in all samples were
181 normalized using *serC* (Jacobs *et al.*, 2012). Error bars indicate standard error of the mean. Black bars,
182 log_2fold-change expression of T3SS regulatory gene *hrpB;* green bars*,* log_2 fold-change expression of
183 T3SS regulatory gene *hrpG;* blue bars*,* log_2 fold-change expression of Type 3-secreted effector gene
184 *ripX.* * $P<0.05$, for qRT, student's t-test compared to gene expression level in untreated WT bacteria; for
185 RNA-seq, FDR using Benjamini-Hochberg.

186

187 **Denitrifying conditions in culture do not replicate *in planta* conditions**

188 Because xylem fluid contains relatively small amounts of nutrients, minimal media has often been
189 considered to mimic the xylem environment (Arlat *et al.*, 1992; Lowe-Power, Hendrich, *et al.*, 2018).

190 Because VDM is a minimal medium and *R. solanacearum* experiences low-oxygen conditions and uses
191 denitrifying respiration during tomato infection, we asked if anaerobic growth in VDM would better mimic
192 the tomato xylem environment than rich media (Dalsing *et al.*, 2015). However, when we examined
193 expression of *R. solanacearum* genes in tomato stems compared to in VDM, we found a total of 1038
194 genes were differentially regulated in these conditions (Supplementary Table 2). Most genes involved in
195 denitrification were expressed at a higher level in VDM than *in planta*. Other broad categories that were
196 altered include sugar metabolism, flagellar motility, amino acid transporters, iron uptake genes, and
197 ribosomal proteins. In line with previous results, T3SS-related genes were among the most highly
198 upregulated genes *in planta* (Jacobs *et al.*, 2012). Overall, growth in VDM did not closely replicate the *in*
199 *planta* environment and the bacterium seemed more reliant on denitrifying metabolism in VDM.
200

201 **Altering denitrification and NO levels causes large gene expression shifts in culture, but minor**
202 **shifts *in planta***

203 To determine if the effects of NO on the T3SS were specific or a part of a general response, we
204 examined genes differentially regulated by altering NO levels chemically and genetically. *In planta*, 187
205 genes were significantly altered by blocking denitrification and NO production in *ΔnarG* while only 49
206 genes were altered in the NO accumulating *ΔnorB*. In *ΔnarG*, nine of the most significantly upregulated
207 genes were directly involved in nitrate sensing and uptake or were components of the nitrate reductase
208 protein, though expression of sulfur metabolic and flagellar assembly genes and the alkanesulfonate
209 uptake protein *ssuB* were also decreased (Supplementary Table 3). When the *ΔnorB* mutant grew *in*
210 *planta*, expression of *ssuB and* some genes involved in chemotaxis and flagellar assembly were
211 decreased relative to the wild-type strain. This muted response highlights the robust regulatory state of *R.*
212 *solanacearum* growing *in planta* and shows that even changes in fundamental aspects of its biology can
213 tolerated (Peyraud *et al.*, 2018).

214 The transcriptomic profiles of the denitrification mutants grown in culture were much more
215 divergent, with 3,145 significantly altered genes in *ΔnarG* and 3,976 altered in *ΔnorB*. In the non-
216 denitrifying *ΔnarG*, the bacterium showed changes in many metabolic pathways, some of which

217 suggested reduced growth and metabolic activity. Down-regulated genes were enriched in KEGG
218 pathways like purine and pyrimidine metabolism, oxidative phosphorylation, and tRNA synthetases
219 (Supplementary Table 3). As also observed *in planta*, *ΔnarG* had reduced expression in genes involved in
220 sulfate and alkanesulfonate uptake and sulfate reduction. *ΔnarG* also had increased expression of
221 flagellar assembly and chemotaxis genes and decreased expression of genes associated with the Sec-
222 dependent secretion and the Type II secretion systems.
223 Genes up-regulated in the NO-accumulating *ΔnorB* mutant were enriched in the KEGG pathways
224 of flagellar assembly, sulfur relay system and fatty acid degradation (Supplementary Table 3).
225 Downregulated genes were enriched in central metabolic KEGG pathways like oxidative phosphorylation,
226 pyrimidine metabolism, biosynthesis of amino acids, and fatty acid biosynthesis. Many of the most highly
227 induced genes were annotated as being involved in either siderophore synthesis or iron uptake, a trend
228 that was also observed in CysNO-treated cells. CysNO-treated *R. solanacearum* cells and *ΔnorB* also
229 saw reduction in expression of Types I, II, and VI secretion systems.
230
231 ***R. solanacearum* encounters more nitrosative stress in VDM than *in planta***
232 To determine the overlap between oxidative and nitrosative stress responses, we examined the
233 expression of genes known to be involved in ROS and RNS responses in *R. solanacearum* and *E. coli*.
234 General ROS-responsive genes included *oxyR*, *katEG*, *sodBC*, *groEL, groES*, *dnaK*, *recA*, *ahpF* and
235 *ahpC1*, *ndh*, *icsA*, *zwf*, *trxA*, and *gor* (Flores-Cruz and Allen, 2009; Flores-Cruz and Allen, 2011). To
236 search for a purely nitrosative response, we looked at the expression of *norB* and *hmpX*, which directly
237 detoxify NO in *R. solanacearum* (Dalsing *et al.*, 2015; Farr and Kogoma, 1991). Transcriptomes of *R.*
238 *solanacearum* cells grown in tomato stems indicated increased oxidative stress *in planta* relative to when
239 growing in VDM. Expression of the *katE* catalase increased 35-fold in wild type bacteria growing in
240 tomato, but *norB* and *hmpX* expression decreased 5-fold and 20-fold, suggesting lower nitrosative stress
241 levels. *In planta*, neither the non-denitrifying *ΔnarG* strain nor the NO overproducing *ΔnorB* strain showed
242 significant changes any known oxidative stress response genes or in *norB* or *hmpX* expression. In
243 culture, our oxidative stress control treatment with H_2O_2 increased expression of *katE*. The H_2O_2 treated

244 cells also had increased expression of NO detoxifying genes *hmpX* and *norB*. The non-denitrifying *ΔnarG*
245 mutant showed changes in most oxidative stress response genes, with decreased expression of a few
246 key genes, such as superoxide dismutase. The NO accumulating *ΔnorB* saw an overall similar trend to
247 *ΔnarG* in its expression of oxidative stress response genes, except it had decreased expression of the
248 chaperones *groES* and *groEL* and increased expression of the iron-sulfur protein *sufA*. As expected, the
249 *ΔnorB* mutant transcriptome suggested NO stress, with an 11-fold up-regulation of the NO-detoxifying
250 *hmpX*. Overall, these results showed some overlap in the response to ROS and RNS stress in culture
251 and suggested that *R. solanacearum in planta* experienced less nitrosative stress in tomato xylem than
252 denitrifying in VDM.
253
254 **Nitric oxide induced expression of T3SS-related genes both *in vitro* and *in planta*.**
255 To determine if in addition to *hrpB*, other T3SS-associated genes are induced by NO in culture,
256 we measured relative expression of all 107 known *R. solanacearum* T3SS genes under each tested
257 condition. These genes encode T3SS structural elements, regulators, secreted effectors, and chaperones
258 (Figure 4, Supplementary Table 4) (Brito *et al.*, 1999; Cunnac *et al.*, 2004; Génin *et al.*, 2005; Van
259 Gijsegem *et al.*, 1995; Lonjon *et al.*, 2015; Lonjon *et al.*, 2017; Marc Marenda *et al.*, 1998; Peeters *et al.*,
260 2013; Plener *et al.*, 2010; Zhang *et al.*, 2011; Y., Zhang *et al.*, 2015; Zhang *et al.*, 2018). Cells of the NO-
261 accumulating *ΔnorB* mutant grown in culture had broadly increased T3SS gene expression relative to wild
262 type, with nine of sixteen structural elements significantly increased. Only one structural element, *hrpF*,
263 trended non-significantly towards reduced expression (Figure 4a). Five out of thirteen known regulators of
264 T3SS were significantly upregulated in *ΔnorB*, although expression of the *prhA*, *prhG*, *prhO*, and the
265 *prhKLM* operon were all reduced. Two out of the four T3E chaperones had significantly elevated
266 expression in *ΔnorB*, as did most T3Es. The differential expression of effectors did not seem to correlate
267 with their known interactions with chaperones (Supplementary table 4). The expression of T3SS genes in
268 CysNO-treated cells largely mirrored that of *norB*, with 80% of tested genes having a similar trend.
269 However, the magnitude of the effect was lower. T3SS gene expression in *ΔnarG* was more varied, with
270 fewer significantly differentially regulated genes than *ΔnorB*. In contrast to *ΔnorB*, *ΔnarG*, and CysNO-

271 treated cultures, H_2O_2-treated cultures had only eight significantly changed T3SS genes (Figure 4a).

272 Overall, we saw a greater induction of T3SS genes in culture by our high-NO conditions than low-NO

273 conditions.

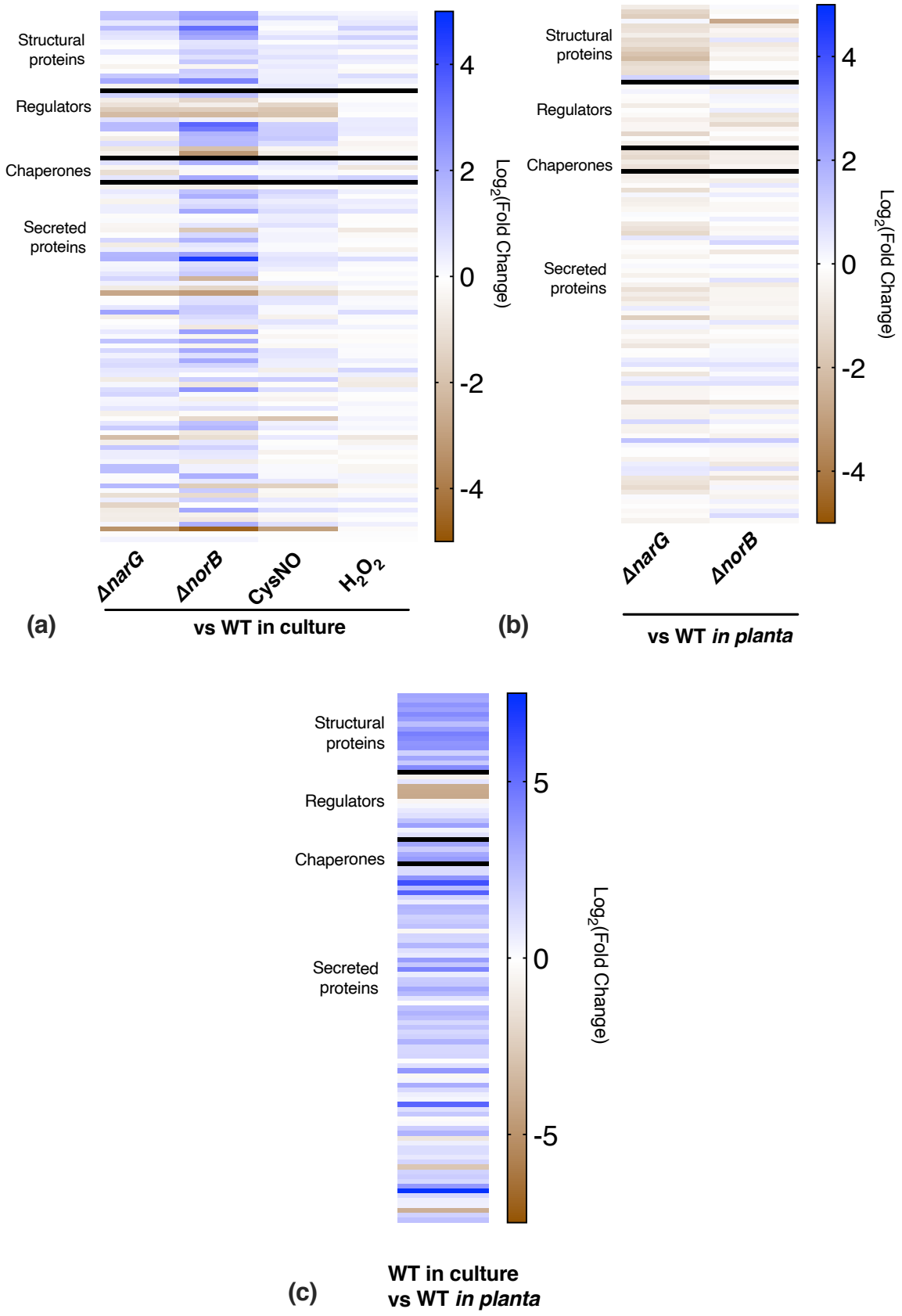
Structural proteins
Regulators
Chaperones
Secreted proteins
ΔnarG
ΔnorB
CysNO
H2O2
(a)
vs WT in culture
4
2
0
-2
-4
Log2(Fold Change)
Structural proteins
Regulators
Chaperones
Secreted proteins
ΔnarG
ΔnorB
(b)
vs WT in planta
4
2
0
-2
-4
Log2(Fold Change)
Structural proteins
Regulators
Chaperones
Secreted proteins
5
0
-5
Log2(Fold Change)
(c)
WT in culture
vs WT in planta

274

275 **Figure 4 Nitric oxide alters expression of T3SS-related genes both *in vitro* and *in planta*. (a)**
276 Heatmap showing relative expression levels of 107 T3SS-associated genes in *R. solanacearum* cells
277 growing in rich medium with varying NO levels. All fold-change numbers are compared to levels in
278 untreated wild-type (WT) cells. Gene annotations, fold change, and significance levels can be found in
279 Supplementary table 4. NO levels were modified genetically using mutants lacking *narG* (deleting this
280 nitrate reductase reduces endogenous NO) and *norB* (deleting this nitric oxide reductase increases
281 endogenous NO). NO levels were increased chemically by adding 1 mM CysNO. Cells treated with 100
282 μM hydrogen peroxide (H_2O_2) were a non-NO control to show general stress responses. **(b)** Relative
283 expression levels of 107 T3SS-associated genes in *R. solanacearum* cells growing *in planta*. About 2000
284 CFU of WT *R. solanacearum, ΔnarG*, or *ΔnorB* were introduced into 17-day old Bonny Best tomato plants
285 through a cut petiole and RNA was harvested from a stem slice 3 days after inoculation. **(c)** Expression of
286 most T3SS-associated genes in *R. solanacearum* strain GMI1000 was enhanced when the bacterium
287 grew in tomato plants relative to when *R. solanacearum* cells multiplied *in vitro* under denitrifying
288 conditions (VDM medium, 0.1% O_2).
289
290 To determine if altering NO levels affects *R. solanacearum* T3SS gene expression in a
291 biologically relevant environment with all natural T3SS regulating inputs, we examined changes in T3SS
292 gene expression in *ΔnarG* and *ΔnorB in planta*. Compared to *R. solanacearum* grown in culture, wild type
293 *R. solanacearum in planta* had much higher expression of almost every T3SS-associated gene (Figure
294 3c). When growing in tomato stems, *ΔnorB* grown *in planta* had no significantly differentially regulated
295 T3SS genes, possibly because relatively high levels of NO are already present in the plant environment
296 (Figure 3b, Supplementary Table 4). In contrast, the non-denitrifying *ΔnarG* mutant showed an overall
297 trend of lower T3SS gene expression, with expression of nine genes significantly reduced (Figure 3b,
298 Supplementary Table 4). Even in the highly T3SS-inducing *in planta* environment, reducing *R.*
299 *solanacearum*-produced NO was sufficient to reduce T3SS gene expression in tomato xylem.
300
301 **Discussion**

302 The T3SS is essential for *R. solanacearum* virulence, as it is for many Gram-negative pathogenic
303 bacteria. Involving at least 16 structural proteins, this secretion system is metabolically expensive to
304 synthesize and operate, so the bacterium is under strong selection pressure to express it only when it
305 increases fitness (Boucher *et al.*, 1985; Genin *et al.*, 1992). Many factors contribute to the regulation of
306 T3SS in *R. solanacearum*, including the presence of undefined host cell wall materials, unknown soluble
307 factors, unknown metabolic cues, and (in culture) quorum sensing (Aldon *et al.*, 2000; Brito *et al.*, 1999;
308 Genin and Denny, 2012; Senuma *et al.*, 2020; Zhang *et al.*, 2011; Zhang *et al.*, 2018; Zuluaga *et al.*,
309 2013). While many T3SS regulators have been described, open questions remain, such as why T3SS is
310 repressed in rich media and whether specific host cell wall components activate PrhA. In addition, many
311 genes that affect T3SS gene expression do so via unknown mechanisms (Zhang *et al.*, 2011; Y., Zhang
312 *et al.*, 2015; Zhang *et al.*, 2018). The results presented here suggests that NO participates in this complex
313 regulatory network.
314 Despite its toxicity at high concentrations, NO is widely used as a signaling molecule in all domains of life
315 (Asgher *et al.*, 2017; Astuti *et al.*, 2018; Simmonds *et al.*, 2014). Many effects of NO are mediated by NO-
316 dependent protein post-translational modifications, including binding transition metals, S-nitrosylation of
317 cysteine, and tyrosine nitration (Cooper, 1999; Kolbert *et al.*, 2017; Leitner *et al.*, 2009; Russwurm and
318 Koesling, 2004; Simmonds *et al.*, 2014; Wünsche *et al.*, 2011; R., Zhang *et al.*, 2015). While most well-
319 characterized mechanisms of NO signaling have been described in eukaryotes, examples of NO signaling
320 in bacteria have also been identified. Species in *Legionella*, *Shewanella*, *Vibrio*, and *Silicibacter* have
321 been shown to use H-NOX proteins to sense NO and regulate biofilm formation (Carlson *et al.*, 2010;
322 Henares *et al.*, 2012; Liu *et al.*, 2012; Network *et al.*, 2012; Rao *et al.*, 2015). NO also contributes to
323 biofilm regulation in *Pseudomonas aeruginosa* via the protein NosP (Hossain and Boon, 2017). Both H-
324 NOX proteins and NosP bind NO using iron centers, but no orthologues of these genes are apparent in
325 the *R. solanacearum* genome. The first example of S-nitrosylation in bacteria was the oxidative stress
326 response protein OxyR in *E. coli* (Seth *et al.*, 2012). OxyR regulates a distinct set of genes when a key
327 cysteine is nitrosylated rather than oxidized. In addition to this, nitrosative stress damage triggers S-
328 nitrosylation of the *Salmonella enterica* redox sensor SsrB and affects the S-nitroso proteome of

329 *Mycobacterium tuberculosis* (Husain *et al.*, 2010; Rhee *et al.*, 2005). Although we show NO activates a
330 key virulence factor in *R. solanacearum*, its specific mechanism of action is not yet known. Using *in silico*
331 predictions of NO-dependent post-translational modifications, we could identify and selectively modify
332 potentially important residues in T3SS regulatory proteins to determine the mechanism of NO-dependent
333 T3SS activation (Liu *et al.*, 2011; Xue *et al.*, 2010).

334 To explore the possibility that the up-regulation by NO of T3SS-associated genes in *R.*
335 *solanacearum* is mediated by S-nitrosylation, we searched for potential S-nitrosylation sites in T3SS
336 regulatory proteins using GPS-SNO (Xue *et al.*, 2010). The strain GMI1000 HrpB protein contains a
337 predicted S-nitrosylation site at cysteine 112 that is conserved across the RSSC and in the corresponding
338 regulatory protein HrpX in plant pathogenic Xanthomonads. However, we were unable to conclusively
339 test this hypothesis since mutating this residue yield ambiguous results (as might be expected for a
340 function regulated by many factors), and we were unable to purify sufficient HrpB protein to chemically
341 measure S-nitrosylation. Thus, this mechanism remains possible but unproven.

342 We found that expression of T3SS-associated genes was enhanced by the presence of a plant
343 host and by exogenous NO released by the NO donor CysNO, and the plant-mediated induction was
344 suppressed by the NO scavenger cPTIO. T3SS gene expression also increased in response to nitric
345 oxide produced by *R. solanacearum* itself, both at natural levels generated by denitrifying respiration and
346 at enhanced levels caused by deleting *norB*. As previously reported (Jacobs *et al.*, 2012; Khokhani *et al.*,
347 2017; Monteiro, Genin, *et al.*, 2012), *R. solanacearum* cells infecting tomato plants highly expressed most
348 T3SS genes, but reducing *R. solanacearum*-produced NO by preventing denitrifying respiration with a
349 Δ*narG* mutation significantly decreased expression of some T3SS-related genes *in planta*. These
350 included genes encoding structural components, HrpF and HrcN, key regulators HrpB and PrhG, the
351 chaperone HpaG, and four T3-secreted effectors. This was especially striking because overall gene
352 expression in *ΔnarG* was otherwise very similar to that of wild type. These results raise the possibility that
353 *R. solanacearum* uses the presence of NO as an indirect indicator of the host xylem environment. There
354 was no increase in T3SS gene expression in the NO-overproducing *ΔnorB* mutant, which may indicate

355 that T3SS genes are already so highly expressed *in planta* that the addition of more NO does not further
356 increase this elevated level of expression.
357 Besides its effects on the T3SS, altering NO concentrations in culture elicited broad changes in
358 gene expression. We reduced NO levels using the non-denitrifying mutant *ΔnarG*. However, preventing
359 the cells from using the denitrification pathway has significant effects on the biology and metabolic state
360 of the cells, making the interpretation of these results challenging. For example, the *ΔnarG* cells grown in
361 culture showed evidence of decreases in growth rate and metabolic activity, indicated by decreased
362 expression in the biosynthetic pathways of nucleotides, reduced expression of the oxidative
363 phosphorylation system, and decreased production of many tRNAs. Treating the cells with NO, either with
364 exogenously applied CysNO or with the NO-overproducing *ΔnorB*, caused similar changes in many
365 metabolic pathways in culture. However, a primary force in culture was the stress caused by increased
366 NO concentrations. This manifested in decreased expression of denitrification and nitrate uptake
367 functions and an increased expression of the NO-detoxifying enzyme *hmpX*. This stress was associated
368 with decreased expression of most *R. solanacearum* secretion systems. However, expression of the
369 T3SS showed the opposite trend, indicating the specificity of NO-dependent T3SS regulation.
370 When denitrification mutants grew *in planta* they had far fewer alterations in gene expression
371 relative to wild type than when the mutants grew in culture. This suggests that inputs from the plant host
372 help *R. solanacearum* control its metabolism and behaviors. Overall, the cells grown *in planta* seem to
373 encounter less nitrosative stress than cells grown in denitrifying conditions in culture. This could mean
374 that NO stress is not as important *in planta* than in culture, but it does not take into account differences in
375 the microenvironments of the xylem environment. Bacteria grown in culture experience a uniform
376 environment with consistent NO stress. In contrast, *R. solanacearum* cells colonizing plant stems occupy
377 multiple different microenvironments, which likely contain varying NO levels.
378 A previous study compared gene expression between *R. solanacearum* grown in rich media and
379 *R. solanacearum* living in tomato xylem (Jacobs *et al*., 2012). Although there were methodological
380 differences between that experiment and this one, we saw many similarities in the DEGs present between
381 in culture and *in planta R. solanacearum*. In both experiments, many of the most highly upregulated

382 genes are involved in the T3SS. Of the genes that were upregulated *in planta* in both experiments, 31 out
383 of 141 (~22%) encoded structural components, regulators, or effectors of the T3SS. Three exceptions to
384 this trend were *prhKLM*. Mutating any of these genes leads to a loss of T3SS gene expression, yet all
385 three were highly downregulated *in planta* compared to either CPG or VDM (Supplementary Table 4)
386 (Jacobs *et al.*, 2012; Zhang *et al.*, 2011). Several other genes that were highly upregulated *in planta* in
387 both experiments encode metabolism of sucrose or myo-inositol, two carbon sources important for *R.*
388 *solanacearum* during infection (Hamilton *et al.*, 2020; Lowe-Power, Khokhani, *et al.*, 2018; Xian *et al.*,
389 2020). Additionally, genes involved in flagellar motility were upregulated in both experiments. A similar
390 number of genes (137) were downregulated *in planta* in both experiments. These included several genes
391 predicted to be involved in amino acid transport and metabolism and the superoxide dismutase genes
392 *sodB* and *sodC*.
393 Components of the denitrification pathway were among the most highly upregulated *R.*
394 *solanacearum* genes *in planta* compared to in rich medium. Consistent with this observation, *R.*
395 *solanacearum* mutants unable to denitrify were reduced in growth *in planta* and in bacterial wilt virulence
396 (Dalsing 2015). However, the same genes were around 20-fold more highly expressed in denitrifying
397 culture than *in planta*. Further, the RNS-responsive NO-detoxifying genes *norB* and *hmpX* were
398 upregulated *in planta* compared to rich media but were expresses much less *in planta* than in denitrifying
399 conditions in culture. This indicates that *Rs* experiences more nitrosative stress when growing in
400 denitrifying culture conditions than when growing in the plant host, which in turn is more nitrosatively
401 stressful than aerobic growth in rich media. These data add to the strong evidence that *R. solanacearum*
402 gene expression and metabolism are very different in the biologically realistic host environment than in
403 culture. This may be due to the complex structure of the xylem environment, where host inputs modulate
404 *R. solanacearum* gene expression, the ability to form defensive biofilms and multiple microenvironments
405 with different nutrient or oxygen concentrations, or because the xylem is a flowing environment,
406 constantly bringing new nutrients into the bacterial habitat. The bacterium's behavior in culture should be
407 regarded as artifactual unless proven otherwise.

408 We attempted to directly measure the concentrations of NO in healthy and infected tomato xylem
409 collected from fluid pooling on a cut stem using the NO-reactive fluorescent dye DAF-FM, electro
410 paramagnetic resonance (EPR), and an NO-sensitive microsensor (Kleschyov *et al.*, 2007; Namin *et al.*,
411 2013; Schreiber *et al.*, 2008; Yoshioka *et al.*, 1996). While a fluorescent signal was observed when DAF-
412 FM was added to xylem sap, no signal was detected through EPR using the NO spin trap cPTIO or with
413 the microsensor (Unisense, Aarhus, Denmark), suggesting that the DAF-FM fluorescence was not
414 specific to NO. These results highlight the need to measure NO using multiple methods in biological
415 systems (Gupta and Igamberdiev, 2013). This failure to detect NO in tomato xylem may not reflect true
416 levels of NO in an intact plant. We collected xylem sap by de-topping tomato plants just above the
417 cotyledons and allowing root pressure to force xylem fluid to pool on the cut stem. Any material exuded in
418 the first two minutes after cutting was removed in an attempt to limit the amount of cellular debris and
419 phloem in the collected material. This method, while useful for obtaining sap to analyze for stable
420 metabolites may not work with a transient metabolite like NO (Lowe-Power, Hendrich, *et al.*, 2018).
421 Cutting the stems stimulates production of reactive oxygen species, which quickly react with NO to form
422 other reactive nitrogen species, potentially diluting any NO signal (Beckman and Koppenol, 1996; Van
423 Faassen and Vanin, 2007; Milling *et al.*, 2011). Furthermore, this approach can only measure NO levels
424 in bulk xylem sap. The xylem is a dynamic and physically heterogenous environment. Xylem flow, xylem
425 structure, and *R. solanacearum*-produced biofilms may all create gradients or microenvironments with
426 altered NO concentrations in the xylem of intact plants (Zimmermann, 1983; Kim *et al.*, 2016; Tran *et al.*,
427 2016; Lowe-Power, Khokhani and Allen, 2018). These factors complicate direct measurement of xylem
428 NO. Confocal microscopy of intact infected stems using fluorescent markers to visualize *R.*
429 *solanacearum*, biofilms, and NO may eventually give a more complete understanding of this challenging
430 landscape.
431 Overall, these results reveal a strong connection between NO levels and expression of the *R.*
432 *solanacearum* T3SS. They suggest that *R. solanacearum* regulates virulence in part by using denitrifying
433 metabolism and the resulting NO as a signal of the hypoxic high-nitrogen host xylem environment.

434 Ongoing work is exploring how *R. solanacearum* manages nitrosative stress and identify additional
435 effects of NO on biology of both host plant and bacterial pathogen.
436
437 **Materials and Methods**
438
439 **Bacterial strains and culture conditions.**
440 All strains, plasmids, and primers used in this study are listed in Supplementary Table 1. *R.*
441 *solanacearum* was cultured in either CPG or a modified VDM medium at 28˚C (Dalsing *et al.*, 2015;
442 Hendrick and Sequeira, 1984). *E. coli* was grown in Luria-Bertani (LB) media at 37˚C. As needed,
443 cultures were supplemented with antibiotics: 25 μg/mL kanamycin or 15 μg/mL gentamicin.
444
445 **Strain construction.**
446 An *R. solanacearum* GMI1000 mutant lacking *hrpB* (RSp0873) was created using a modified
447 *sacB*-dependent positive selection vector, pUFR80 (Castañeda *et al.*, 2005). The regions directly
448 upstream and downstream of *hrpB* were amplified using the ΔhrpBup/dwn primer pairs. These fragments
449 were then inserted into pUFR80 digested with *Hind*III using Gibson assembly (Sievers *et al.*, 2011). The
450 resulting plasmid, pUFR80-ΔhrpB was transformed into *R. solanacearum* GMI1000 and successful
451 plasmid integrations were selected for kanamycin resistance. The resulting colonies were then counter
452 selected on CPG + 5% w/v sucrose. Successful deletions were confirmed using PCR, sequencing, and a
453 functional screen for the ability to induce HR on the incompatible host *N. tabacum* (Poueymiro *et al.*,
454 2009).
455 The *ΔhrpB* mutation was complemented by inserting a DNA fragment encoding *hrpB* and *hrcC*
456 with the ~600 bp upstream containing their native promoter into the selectively neutral *att* site in the *R.*
457 *solanacearum* chromosome using pRCK (Monteiro, Solé, *et al.*, 2012). The fragment was amplified using
458 hrpBcomp_F/R and inserted into *AvRII/XbaI*-digested pRCK using Gibson assembly. This vector was
459 then transformed into *ΔhrpB* and selected on CPG+kan.
460

461 **Plant growth conditions.**

462 Wilt-susceptible tomato cv. Bonny Best were germinated and grown in BM2 all-purpose
463 germination and propagation mix (Berger, Saint-Modeste, QC). Plants were grown at 28˚C with a 12 hr
464 photoperiod. Seedlings were transplanted after 14 days. After transplanting, plants were watered on
465 alternate days with 1/2 strength Hoagland solution. Tomato seeds for axenic seedling production were
466 sterilized by washing with 10% bleach for ten minutes, followed by two five-minute washes in 70%
467 ethanol, then rinsed five times with water and germinated on water agar plates.

468

469 **Lux reporter assays.**

470 To test the effect of denitrification on T3SS gene expression, *R. solanacearum* strain GMI1000
471 carrying a *hrpB::lux* reporter gene fusion was grown in denitrifying conditions as follows (Monteiro, Genin,
472 *et al.*, 2012). Overnight cultures grown in CPG were resuspended in VDM with or without 30 mM
473 potassium nitrate to an initial OD_{600} of 0.001. These cultures were grown in 200 μL volumes in clear-
474 bottomed white-walled 96 well plates at 28˚C in 0.1% O_2 with shaking. Every half hour, the Abs_{600} and
475 luminescence was measured using a BioTek SynergyHT microplate reader (BioTek, Winooski, VT, USA).
476 To determine the effects of the NO scavenger cPTIO on T3SS gene expression, *hrpB::lux* cultures were
477 resuspended in 24-well plates in 1 mL of water, either with or without two five day-old sterile tomato
478 seedlings. As appropriate, cPTIO was added to a final concentration of 1 mM. The plates were incubated
479 at 28˚C with shaking for ~24 hours. The pigmented liquid was removed from the seedlings and
480 transferred to 1.5 mL Eppendorf tubes, after which the bacteria were pelleted by centrifugation. The
481 pigmented supernatant was removed, and the pellets resuspended in 200 μL of water. These
482 suspensions were transferred to a new plate and the Abs_{600} and luminescence was measured as detailed
483 above.

484

485 **RNA extraction for sequencing**.

486 To profile gene expression of *R. solanacearum* at various levels of NO stress, we extracted RNA
487 from *R. solanacearum* grown in culture and *in planta*. For each in condition, we used *R. solanacearum*

488 from three separate overnight cultures as biological replicates. For the *in vitro* samples, overnight cultures
489 grown in CPG were resuspended to a final OD_{600} of 0.01 in 50 mL of VDM + 30 mM potassium nitrate in
490 conical tubes. These cultures were incubated without shaking for 12 hours at 28˚C in 0.1% O_2. Four hours
491 before harvesting, CysNO or H_2O_2 were added to the relevant cultures to a final concentration of 1 mM
492 and 100 μM, respectively. CysNO was synthesized by adding HCl to a solution containing 200 mM L-
493 cysteine and 200 mM sodium nitrite. The solution was incubated in the dark for ten minutes before it was
494 neutralized by adding sodium hydroxide to a final concentration of 200 mM. The molarity of the solution
495 was determined using the absorbance at 334 nm and the extinction coefficient 90/M*cm. After 16h total
496 incubation, sub-samples were collected for dilution plating to determine CFU/ml and the tubes were
497 capped and centrifuged at room temperature for 5 min at 8000 rpm. The supernatant was removed and
498 pellets were frozen in liquid nitrogen. RNA extractions were carried out using a modified version of the
499 Quick-RNA™ MiniPrep kit (Zymo Research, Irvine, CA, USA), as follows. Pellets were resuspended in
500 400 μL of ice cold TE pH 8 with 1 mg/mL lysozyme, 0.25 μL Superase Inhibitor (Ambion, Austin, TX,
501 USA), and 80 μL of 10% SDS, vortexed for 10s, transferred to a new 2 mL tube, and shaken at ~300 rpm
502 for 2 min. 800 μL of RNA-Lysis lysis buffer was added, the tubes were vortexed again for 10 s, cleaned
503 according to the kit manufacturer's instructions, and eluted in 100 μL of water. Nucleic acid
504 concentrations were estimated using a nanodrop, normalized to 200 ng/uL, and cleaned using the DNA-
505 free DNAse kit (Invitrogen, Carlsbad, CA, USA). Samples were incubated at 37C for 1 hour, with 2 μL
506 more of DNAse added at 30 min. After DNAse inactivation, samples were further cleaned by chloroform
507 extraction, then precipitated overnight at -20˚C with 100 μM Sodium Acetate pH 5.5 and 66 % ethanol.
508 Samples were checked for concentration on a Nanodrop, for DNA contamination by PCR using the qRT-
509 PCR primers *serC*_F/R, and for RNA integrity (RIN) using an Agilent Bioanalyzer 21000 (Agilent, Santa
510 Clara, CA, USA). All samples had RIN values above 7.3.

511 The *in planta* samples were harvested after 21 day old Bonny Best tomatoes were inoculated with
512 ~2000 CFU of each bacteria strain through the cut petiole of the first true leaf. At 3 dpi, approximately 0.1
513 g of stem tissue was collected from the site of inoculation, immediately frozen in liquid nitrogen, and
514 stored at -80˚C. Another ~0.1 g of tissue was collected from directly below the inoculation site and was

515 ground in bead beater tubes using a PowerLyzer (Qiagen, Hilden, Germany) for two cycles of 2200 rpm
516 for 90 s in each with a 4 min rest between cycles. This material was then dilution plated to measure
517 bacterial colonization. From each biological replicate, we chose six plants with the most similar level of
518 colonization. RNA was extracted from these using a modified hot phenol-chloroform method (Jacobs *et*
519 *al*., 2012). Between 4 and 5 individual plants were pooled per biological replicate. Nucleic acid sample
520 quality was checked using a nanodrop, Agilent bioanalyzer, and qRT-PCR primers Actin_F/R. All samples
521 had RIN values of above 7.2.
522
523 **RNA sequencing and data analysis.**
524 All RNA was sent to Novogene (Beijing, China) for library preparation, sequencing, and analysis.
525 rRNA depletion, fragmentation, and library construction were done using NEBNext® *μ*Ltra™ Directional
526 RNA Library Prep Kit for Illumina® (NEB, Ipswitch, MA, USA) following the manufacturer's
527 recommendation and starting with 3 μg of RNA per sample. After the libraries were constructed, their
528 quality was assessed using an Agilent Bioanalyzer 21000 system and sequenced using an Illumina
529 platform to generate paired-end reads. Between 19,000,000 and 40,000,000 reads were produced per
530 sample. Raw reads were converted to FASTQ files using Illumina CASAVA v1.8, and then filtered for
531 quality, removing reads with adaptor contamination, greater than 10% uncertain nucleotides, or more than
532 50% of nucleotides with a Q_{pred} less than or equal to 5. Over 95% of reads were of good quality, and were
533 mapped to the *R. solanacearum* GMI1000 genome
534 (https://www.ncbi.nlm.nih.gov/assembly/GCF_000009125.1) using Bowtie2 -2.2.3 (Langmead *et al*.,
535 2009). From this, gene expression was calculated using HTseq v0.6.1 and differential gene expression
536 was calculated using DESeq 1.18.0. P-values calculated by DESeq were adjusted to control for the false
537 discovery rate (FDR) using the Benjamini-Hochberg approach. Gene Ontology enrichment was analyzed
538 using GOseq Release2.12 and KEGG enrichment was calculated using KOBAS v2.0 software.
539
540 **Measuring T3SS expression with qRT-PCR.**

541 Expression of T3SS genes was measured in denitrification mutants grown in 40 mL of VDM + 30
542 mM nitrate grown in GasPak™ EZ microaerobic pouches (BD, Franklin Lakes, NJ, USA) at 28˚C with
543 shaking for 18 hours starting from an OD_{600} of 0.001. RNA extractions were carried out using a hot
544 phenol-chloroform method(Jacobs *et al.*, 2012). Extractions were carried out using the Quick-RNA™
545 MiniPrep kit (Zymo Research, Irvine, CA, USA). cDNA synthesis was done using the Superscript VILO
546 cDNA synthesis kit (Invitrogen, Carlsbad, CA, USA). qPCR reactions were carried out in 10 μL volumes
547 using 5 ng of total template using PowerUp Syber Green Master) in a QuantStudio 5 Real-Time PCR
548 System Mix (Applied Biosystems, Foster City, CA, USA).
549

550 **Acknowledgments**

551 The authors would like to thank Jon Jacobs for discussion and advice throughout the project and Max
552 Miao for his expertise and discussion about statistics and R. This work was funded by National Sciences
553 Foundation grant IOS 1258082. CGH and BLD were supported by NSF predoctoral fellowships. This
554 material is based upon work supported by the National Science Foundation Graduate Research
555 Fellowship Program under Grant No. DGE-1747503. Any opinions, findings, and conclusions or
556 recommendations expressed in this material are those of the author(s) and do not necessarily reflect the
557 views of the National Science Foundation. The authors declare no competing financial interests
558

559 **Data Availability Statement**

560 The data supporting this research are openly available in the Gene Expression Omnibus at
561 https://www.ncbi.nlm.nih.gov/geo/query/acc.cgi?acc=GSE160024, GEO accession: GSE160024.
562

563 **References**

564

565 **Aldon, D., Brito, B., Boucher, C. and Genin, S.** (2000) A bacterial sensor of plant cell contact controls
566 the transcriptional induction of *Ralstonia solanacearum* pathogenicity genes. *Embo J.* **19**, 2304–
567 2314.

568 **Arlat, M., Gough, C.L., Zischek, C., Barberis, P. a, Trigalet, A. and Boucher, C. a** (1992)
569 Transcriptional organization and expression of the large hrp gene cluster of *Pseudomonas*
570 *solanacearum*. *Mol. Plant. Microbe. Interact.* **5**, 187–193.
571 **Asgher, M., Per, T.S., Masood, A., Fatma, M., Freschi, L., Corpas, F.J. and Khan, N.A.** (2017) Nitric
572 oxide signaling and its crosstalk with other plant growth regulators in plant responses to abiotic
573 stress. *Environ. Sci. Pollut. Res.* **24**, 2273–2285.
574 **Astuti, R.I., Nasuno, R. and Takagi, H.** (2018) Nitric Oxide Signalling in Yeast. *Adv. Microb. Physiol.* **72**,
575 29–63.
576 **Beckman, J.S. and Koppenol, W.H.** (1996) Nitric oxide, superoxide, and peroxynitrite: the good, the
577 bad, and ugly. *Am. J. Physiol.* **271**, C1424-37.
578 **Boucher, C.A., Barberis, P.A., Trigalet, A.P. and Demery, D.A.** (1985) Transposon mutagenesis of
579 *Pseudomonas solanacearum*: Isolation of Tn5-induced avirulent mutants. *J. Gen. Microbiol.* **131**,
580 2449–2457.
581 **Brito, B., Marenda, M. and Barberis, P.** (1999) *prhJ* and *hrpG*, two new components of the plant signal-
582 dependent regulatory cascade controlled by PrhA in *Ralstonia solanacearum*. *Mol. Microbiol.* **31**,
583 237–251.
584 **Carlson, H.K., Vance, R.E. and Marletta, M.A.** (2010) H-NOX Regulation of c-di-GMP Metabolism and
585 Biofilm Formation in *Legionella pneumophila*. *Mol. Microbiol.* **77**, 930–942.
586 **Castañeda, A., Reddy, J., El-Yacoubi, B. and Gabriel, D.** (2005) Mutagenesis of all eight *avr* genes in
587 *Xanthomonas campestris* pv. *campestris* had no detected effect on pathogenicity, but one *avr* gene
588 affected race specificity. *Mol. Plant-Microbe Interact.* **18**, 1306–1317.
589 **Cooper, C.E.** (1999) Nitric oxide and iron proteins. *Biochim. Biophys. Acta - Bioenerg.* **1411**, 290–309.
590 **Cunnac, S., Occhialini, A., Barberis, P., Boucher, C. and Genin, S.** (2004) Inventory and functional
591 analysis of the large Hrp regulon in *Ralstonia solanacearum*: identification of novel effector proteins
592 translocated to plant host cells through the type III secretion system. *Mol. Microbiol.* **53**, 115–128.
593 **Dalsing, B.L., Truchon, A.N., Gonzalez-Orta, E.T., Milling, A.S. and Allen, C.** (2015) *Ralstonia*
594 *solanacearum* uses inorganic nitrogen metabolism for virulence, ATP production, and detoxification

595 in the oxygen-limited host xylem environment. *MBio* **6**, 1–13.

596 **Delledonne, M., Xia, Y., Dixon, R. a and Lamb, C.** (1998) Nitric oxide functions as a signal in plant
597 disease resistance. *Nature* **394**, 585–588.

598 **Elphinstone, J.** (2005) The current bacterial wilt situation: a global overview. In Bacterial Wilt: The
599 Disease and the *Ralstonia solanacearum* Species Complex. (Allen, C., Prior, P., and Hayward, A.C.,
600 eds), pp. 9–28. St Paul, MN: Society, American Phytopathological.

601 **Faassen, E. Van and Vanin, A.F.** (2007) Nitric oxide radicals and their reactions, Elsevier B.V.

602 **Farr, S.B. and Kogoma, T.** (1991) Oxidative stress responses in *Escherichia coli* and *Salmonella*
603 *typhimurium*. *Microbiol. Rev.* **55**, 561–585.

604 **Flores-Cruz, Z. and Allen, C.** (2011) Necessity of OxyR for the hydrogen peroxide stress response and
605 full virulence in *Ralstonia solanacearum*. *Appl. Environ. Microbiol.* **77**, 6426–6432.

606 **Flores-Cruz, Z. and Allen, C.** (2009) *Ralstonia solanacearum* Encounters an Oxidative Environment
607 During Tomato Infection. *MPMI*, 773–782.

608 **Ge, S.X., Son, E.W. and Yao, R.** (2018) iDEP: An integrated web application for differential expression
609 and pathway analysis of RNA-Seq data. *BMC Bioinformatics* **19**, 1–24.

610 **Génin, S., Brito, B., Denny, T.P. and Boucher, C.** (2005) Control of the *Ralstonia solanacearum* Type III
611 secretion system (Hrp) genes by the global virulence regulator PhcA. *FEBS Lett.* **579**, 2077–2081.

612 **Genin, S. and Denny, T.P.** (2012) Pathogenomics of the *Ralstonia solanacearum* species complex.
613 *Annu. Rev. Phytopathol.* **50**, 67–89.

614 **Genin, S., Gough, C.L., Zischek, C. and Boucher, C.A.** (1992) Evidence that the hrpB gene encodes a
615 positive regulator of pathogenicity genes from *Pseudomonas solanacearum*. *Mol. Microbiol.* **6**,
616 3065–3076.

617 **Gijsegem, F. Van, Gough, C., Zischek, C., et al.** (1995) The hrp gene locus of *Pseudomonas*
618 *solanacearum*, which controls the production of a type III secretion system, encodes eight proteins
619 related to components of the bacterial flagellar biogenesis complex. *Mol. Microbiol.* **15**, 1095–1114.

620 **Gupta, K.J. and Igamberdiev, A.U.** (2013) Recommendations of using at least two different methods for
621 measuring NO. *Front. Plant Sci.* **4**, 2–5.

622 **Hamilton, C.D., Steidl, O.R., Macintyre, A.M., Hendrich, C.G. and Allen, C.** (2020) *Ralstonia*
623 *solanacearum* depends on catabolism of myo-inositol, sucrose, and trehalose for virulence in an
624 infection stage-dependent manner. *MPMI*.
625 **Hanahan, D.** (1983) Studies on Transformation of *Escherichia coli* with Plasmids. *J. Mol. Biol.* **166**, 557–
626 580.
627 **Henares, B.M., Higgins, K.E. and Boon, E.M.** (2012) Discovery of a Nitric Oxide Responsive Quorum
628 Sensing Circuit in *Vibrio harveyi*. *ACS Chem. Biol.* **7**, 1331–1336.
629 **Hendrick, C.A. and Sequeira, L.** (1984) Lipopolysaccharide-defective mutants of the wilt pathogen
630 *Pseudomonas solanacearum*. *Appl. Environ. Microbiol.* **48**, 94–101.
631 **Hossain, S. and Boon, E.M.** (2017) Discovery of a Novel Nitric Oxide Binding Protein and Nitric-Oxide-
632 Responsive Signaling Pathway in *Pseudomonas aeruginosa*. *ACS Infect. Dis.* **3**, 454–461.
633 **Husain, M., Jones-carson, J., Song, M., Mccollister, B.D. and Bourret, T.J.** (2010) Redox sensor SsrB
634 Cys 203 enhances *Salmonella* fitness against nitric oxide generated in the host immune response to
635 oral infection. *Proc Natl Acad Sci U S A* **107**, 4–13.
636 **Jacobs, J.M., Babujee, L., Meng, F., Milling, A.S. and Allen, C.** (2012) The *in planta* transcriptome of
637 *Ralstonia solanacearum*: conserved physiological and virulence strategies during bacterial wilt of
638 tomato. *MBio* **3**, e00114-12.
639 **Khokhani, D., Lowe-Power, T.M., Tran, T.M. and Allen, C.** (2017) A Single Regulator Mediates
640 Strategic Switching between Attachment / Spread and Growth / Virulence in the Plant Pathogen
641 *Ralstonia solanacearum*. *MBio* **8**, 1–20.
642 **Kim, M.K., Ingremeau, F., Zhao, A., Bassler, B.L. and Stone, H.A.** (2016) Local and global
643 consequences of flow on bacterial quorum sensing. *Nat. Microbiol.* **1**, 15005.
644 **Kleschyov, A.L., Wenzel, P. and Munzel, T.** (2007) Electron paramagnetic resonance (EPR) spin
645 trapping of biological nitric oxide. *J. Chromatogr. B Anal. Technol. Biomed. Life Sci.*
646 **Kolbert, Z., Feigl, G., Bordé, Á., Molnár, Á. and Erdei, L.** (2017) Protein tyrosine nitration in plants:
647 Present knowledge, computational prediction and future perspectives. *Plant Physiol. Biochem.* **113**,
648 56–63.

649 **Langmead, B., Trapnell, C., Pop, M. and Salzberg, S.L.** (2009) Ultrafast and memory-efficient
650 alignment of short DNA sequences to the human genome. *Genome Biol.* **10**.
651 **Leitner, M., Vandelle, E., Gaupels, F., Bellin, D. and Delledonne, M.** (2009) NO signals in the haze.
652 Nitric oxide signalling in plant defence. *Curr. Opin. Plant Biol.* **12**, 451–458.
653 **Liu, N., Xu, Y., Hossain, S., Huang, N., Coursolle, D. and Gralnick, J.A.** (2012) Nitric Oxide Regulation
654 of Cyclic di-GMP Synthesis and Hydrolysis in *Shewanella woodyi*. *Biochemistry* **51**, 2087–2099.
655 **Liu, Z., Cao, J., Ma, Q., Gao, X., Ren, J. and Xue, Y.** (2011) GPS-YNO2: computational prediction of
656 tyrosine nitration sites in proteins. *Mol. Biosyst.* **7**, 1197.
657 **Lonjon, F., Lohou, D., Cazalé, A.C., Büttner, D., Ribeiro, B.G., Péanne, C., Genin, S. and Vailleau, F.**
658 (2017) HpaB-Dependent Secretion of Type III Effectors in the Plant Pathogens *Ralstonia*
659 *solanacearum* and *Xanthomonas campestris* pv. *vesicatoria*. *Sci. Rep.* **7**, 1–14.
660 **Lonjon, F., Turner, M., Henry, C., et al.** (2015) Comparative Secretome Analysis of *Ralstonia*
661 *solanacearum* Type 3 Secretion-Associated Mutants Reveals a Fine Control of Effector Delivery,
662 Essential for Bacterial Pathogenicity. *Mol. Cell. Proteomics*.
663 **Lowe-Power, T.M., Hendrich, C.G., Roepenack-Lahaye, E. von, et al.** (2018) Metabolomics of tomato
664 xylem sap during bacterial wilt reveals *Ralstonia solanacearum* produces abundant putrescine, a
665 metabolite that accelerates wilt disease. *Environ. Microbiol.* **20**, 1330–1349.
666 **Lowe-Power, T.M., Khokhani, D. and Allen, C.** (2018) How *Ralstonia solanacearum* Exploits and
667 Thrives in the Flowing Plant Xylem Environment. *Trends Microbiol.* **26**, 929–942.
668 **Marc Marenda, Callard, B.B.D., Genin, S., Barberis, P., Boucher, C. and Arlat, M.** (1998) PrhA
669 controls a novel regulatory pathway required for the specific induction of *Ralstonia solanacearum*
670 *hrp* genes in the presence of plant cells. *Mol. Microbiol.* **27**, 437–453.
671 **Milling, A.S., Babujee, L. and Allen, C.** (2011) *Ralstonia solanacearum* extracellular polysaccharide is a
672 specific elicitor of defense responses in wilt-resistant tomato plants. *PLoS One* **6**.
673 **Monteiro, F., Genin, S., Dijk, I. van and Valls, M.** (2012) A luminescent reporter evidences active
674 expression of *Ralstonia solanacearum* type III secretion system genes throughout plant infection.
675 *Microbiol. (United Kingdom)* **158**, 2107–2116.

676 **Monteiro, F., Solé, M., Dijk, I. van and Valls, M.** (2012) A chromosomal insertion toolbox for promoter
677 probing, mutant complementation, and pathogenicity studies in *Ralstonia solanacearum*. *Mol. Plant.*
678 *Microbe. Interact.* **25**, 557–68.
679 **Namin, S.M., Nofallah, S., Joshi, M.S., Kavallieratos, K. and Tsoukias, N.M.** (2013) Kinetic analysis of
680 DAF-FM activation by NO: Toward calibration of a NO-sensitive fluorescent dye. *Nitric Oxide - Biol.*
681 *Chem.* **28**, 39–46.
682 **Network, C.S., Plate, L. and Marletta, M.A.** (2012) Article Nitric Oxide Modulates Bacterial Biofilm
683 Formation through a Multicomponent. *Mol. Cell* **46**, 449–460.
684 **Peeters, N., Carrère, S., Anisimova, M., Plener, L., Cazalé, A.-C. and Genin, S.** (2013) Repertoire,
685 unified nomenclature and evolution of the Type III effector gene set in the *Ralstonia solanacearum*
686 species complex. *BMC Genomics* **14**, 859.
687 **Peyraud, R., Cottret, L., Marmiesse, L. and Genin, S.** (2018) Control of primary metabolism by a
688 virulence regulatory network promotes robustness in a plant pathogen. *Nat. Commun.* **9**, 418.
689 **Pfeiffer, S., Leopold, E., Hemmens, B., Schmidt, K., Werner, E.R. and Mayer, B.** (1997) Interference
690 of carboxy-PTIO with nitric oxide-and peroxynitrite- mediated reactions. *Free Radic. Biol. Med.* **22**,
691 787–794.
692 **Plener, L., Manfredi, P., Valls, M. and Genin, S.** (2010) PrhG, a transcriptional regulator responding to
693 growth conditions, is involved in the control of the type III secretion system regulon in *Ralstonia*
694 *solanacearum*. *J. Bacteriol.* **192**, 1011–1019.
695 **Poueymiro, M., Cunnac, S., Barberis, P., Deslandes, L., Peeters, N., Cazale-Noel, A.-C., Boucher, C.**
696 **and Genin, S.** (2009) Two Type III Secretion System Effectors from *Ralstonia solanacearum*
697 GMI1000 Determine Host-Range Specificity on Tobacco. *Mol. Plant-Microbe Interact.* **22**, 538–550.
698 **Poueymiro, M. and Genin, S.** (2009) Secreted proteins from *Ralstonia solanacearum*: a hundred tricks
699 to kill a plant. *Curr. Opin. Microbiol.* **12**, 44–52.
700 **Rao, M., Smith, B.C. and Marletta, M.A.** (2015) Nitric Oxide mediates biofilm formation and symbiosis in
701 *Silicibacter* sp. strain TrichCH4B. *MBio* **6**, 1–10.
702 **Rhee, K.Y., Erdjument-Bromage, H., Tempst, P. and Nathan, C.F.** (2005) S-nitroso proteome of

703 *Mycobacterium tuberculosis*: Enzymes of intermediary metabolism and antioxidant defense. *Proc.*
704 *Natl. Acad. Sci. U. S. A.* **102**, 467–72.
705 **Russwurm, M. and Koesling, D.** (2004) NO activation of guanylyl cyclase. *EMBO J.* **23**, 4443–4450.
706 **Scheler, C., Durner, J. and Astier, J.** (2013) Nitric oxide and reactive oxygen species in plant biotic
707 interactions. *Curr. Opin. Plant Biol.* **16**, 534–539.
708 **Schreiber, F., Polerecky, L. and Beer, D. De** (2008) Nitric oxide microsensor for high spatial resolution
709 measurements in biofilms and sediments. *Anal. Chem.* **80**, 1152–1158.
710 **Senuma, W., Takemura, C., Hayashi, K., Ishikawa, S., Kiba, A., Ohnishi, K., Kai, K. and Hikichi, Y.**
711 (2020) The putative sensor histidine kinase PhcK is required for the full expression of *phcA*
712 encoding the global transcriptional regulator to drive the quorum-sensing circuit of *Ralstonia*
713 *solanacearum* strain OE1-1. *Mol. Plant Pathol.*, 1–15.
714 **Seth, D., Hausladen, A., Wang, Y.-J. and Stamler, J.S.** (2012) Endogenous Protein S-Nitrosylation in *E.*
715 *coli*: Regulation by OxyR. *Science (80-.).* **336**, 470–3.
716 **Sievers, F., Wilm, A., Dineen, D., et al.** (2011) Fast, scalable generation of high-quality protein multiple
717 sequence alignments using Clustal Omega. *Mol. Syst. Biol.* **7**, 539–545.
718 **Simmonds, M.J., Detterich, J.A. and Connes, P.** (2014) Nitric oxide, vasodilation and the red blood cell.
719 *Biorheology* **51**, 121–134.
720 **Simontacchi, M., Galatro, A., Ramos-Artuso, F. and Santa-María, G.E.** (2015) Plant Survival in a
721 Changing Environment: The Role of Nitric Oxide in Plant Responses to Abiotic Stress. *Front. Plant*
722 *Sci.* **6**, 977.
723 **Swanson, J.K., Montes, L., Mejia, L. and Allen, C.** (2007) Detection of latent infections of *Ralstonia*
724 *solanacearum* race 3 biovar 2 in geranium. *Plant Dis.* **91**, 828–834.
725 **Tran, T., MacIntyre, A., Khokhani, D., Hawes, M.C. and Allen, C.** (2016) Extracellular DNases of
726 *Ralstonia solanacearum* modulate biofilms and facilitate bacterial wilt virulence. *Environ. Microbiol.*
727 *Environ. Microbiol. Reports* **00**, 1–15.
728 **Vasse, J., Frey, P. and Trigalet, A.** (1994) Microscopic studies of intercellular infection and protoxylem
729 invasion of tomato roots by *Pseudomonas solanacearum*. *MPMI* **8**, 241–251.

730 **Wilson, I.D., Neill, S.J. and Hancock, J.T.** (2008) Nitric oxide synthesis and signalling in plants. *Plant,*
731 *Cell Environ.* **31**, 622–631.
732 **Wünsche, H., Baldwin, I.T. and Wu, J.** (2011) S-Nitrosoglutathione reductase (GSNOR) mediates the
733 biosynthesis of jasmonic acid and ethylene induced by feeding of the insect herbivore *Manduca*
734 *sexta* and is important for jasmonate-elicited responses in *Nicotiana attenuata*. *J. Exp. Bot.* **62**,
735 4605–4616.
736 **Xian, L., Yu, G., Wei, Y., Rufian, J.S., Li, Y., Zhuang, H., Xue, H., Morcillo, R.J.L. and Macho, A.P.**
737 (2020) A Bacterial Effector Protein Hijacks Plant Metabolism to Support Pathogen Nutrition. *Cell*
738 *Host Microbe*, 1–10.
739 **Xue, Y., Liu, Z., Gao, X., Jin, C., Wen, L., Yao, X. and Ren, J.** (2010) GPS-SNO: Computational
740 prediction of protein s-nitrosylation sites with a modified GPS algorithm. *PLoS One* **5**, 1–7.
741 **Yoshioka, T., Iwamoto, N. and Ito, K.** (1996) An application of electron paramagnetic resonance to
742 evaluate nitric oxide and its quenchers. *J. Am. Soc. Nephrol.* **7**, 961–965.
743 **Yuliar, Nion, Y.A. and Toyota, K.** (2015) Recent trends in control methods for bacterial wilt diseases
744 caused by *Ralstonia solanacearum*. *Microbes Environ.* **30**, 1–11.
745 **Zhang, R., Hess, D.T., Qian, Z., Hausladen, A., Fonseca, F., Chaube, R., Reynolds, J.D. and**
746 **Stamler, J.S.** (2015) Hemoglobin βCys93 is essential for cardiovascular function and integrated
747 response to hypoxia. *Proc. Natl. Acad. Sci. U. S. A.* **112**, 6425–6430.
748 **Zhang, Y., Kiba, A., Hikichi, Y. and Ohnishi, K.** (2011) prhKLM genes of *Ralstonia solanacearum*
749 encode novel activators of hrp regulon and are required for pathogenesis in tomato. *FEMS*
750 *Microbiol. Lett.* **317**, 75–82.
751 **Zhang, Y., Li, J., Zhang, W., Shi, H., Luo, F., Hikichi, Y., Shi, X. and Ohnishi, K.** (2018) A putative
752 LysR-type transcriptional regulator PrhO positively regulates the type III secretion system and
753 contributes to the virulence of *Ralstonia solanacearum*. *Mol. Plant Pathol.*, 1–12.
754 **Zhang, Y., Luo, F., Wu, D., Hikichi, Y., Kiba, A., Igarashi, Y., Ding, W. and Ohnishi, K.** (2015) PrhN, a
755 putative marR family transcriptional regulator, is involved in positive regulation of type III secretion
756 system and full virulence of *Ralstonia solanacearum*. *Front. Microbiol.* **6**, 1–12.

757 **Zimmermann, M.H.** (1983) Xylem Structure and the Ascent of Sap, Berlin: Springer-Verlag.

758 **Zuluaga, A.P., Puigvert, M. and Valls, M.** (2013) Novel plant inputs influencing *Ralstonia solanacearum*

759 during infection. *Front. Microbiol.* **4**, 1–7.

760

761

762 **Supplementary Materials**

763

764 **Supplementary Table 1 – Bacterial strains, plasmids, and primers**

765

Strains	**Relevant characteristics**	**Reference**
R. solanacearum		
GMI1000	Phylotype I seq 18 strain isolated from tomato in French Guyana	(Boucher *et al.*, 1985)
hrpB::lux	GMI1000 expressing the bacterial *lux* reporter controlled by the *hrpB* promoter, Kan^R	(Monteiro, Genin, *et al.*, 2012)
ΔnarG	GMI1000 lacking *narG*, a nitrate reductase. Cannot denitrify and does not produce NO, Gm^R	(Dalsing *et al.*, 2015)
ΔnorB	GMI1000 lacking *norB*, a nitric oxide reductase. Can denitrify, but accumulates NO, Gm^R	(Dalsing *et al.*, 2015)
ΔhrpB	GMI1000 lacking *hrpB*. Avirulent and does not express a T3SS	This study
hrpB comp	*ΔhrpB* complemented.,Kan^R	This study
E. coli		
DH5α	dlacZ, Delta M15 Delta(lacZYA-argF) U169 recA1 endA1 hsdR17(rK-mK+) supE44 thi-1 gyrA96 relA1	(Hanahan, 1983)
Plasmid	**Description**	**Reference**
pUFR80	Positive sucrose selection vector, Suc^S, Kan^R	(Castañeda *et al.*, 2005)
pRCK-GWY	Gateway destination vector that integrates into the GMI1000 genome at the neutral *att* site; Kan^R	(Monteiro, Solé, *et al.*, 2012)
pUFR80-ΔhrpB	Vector used to make unmarked *R. solanacearum ΔripB*, Suc^S, Kan^R	This study
pRCK-hrpBcomp	Complementation vector containing WT *hrpB* and *hrcC*, Kan^R	This study
Cloning Primers		
Primer	**Sequence[a]**	**Reference**
ΔhrpBup_F	5' – cgacggccagtgccaGTTCGATACCAGCGAAAGC target locus: RSp0873	This study
ΔhrpBup_R	5' – cggagggcGGCAATGCTCCTGAAGCG target locus: RSp0873	This study
ΔhrpBdwn_F	5' – gcattgccGCCCTCCGGCGGACCGCC target locus: RSp0873	This study
ΔhrpBdwn_R	5' – acctgcaggcatgcaGCTGTTGCCGACGTATTGACCGGTGC target locus: RSp0873	This study
hrpBcomp_F	5' – tgcgcgagcaggggaattgcGACAACGTCTCCGGGTTC target locus: RSp0873-RSp0874	This study
hrpBcomp_R	5' – cgaccctagtctaagatcttCTTCGGCATTCGGCAATG target locus: RSp0873-RSp0874	This study
qRT-PCR Primers		
Primer	**Sequence**	**Reference**
hrpB_F	5' – CCTGCCCGAATACGCAAATG target locus: RSp0873	This study
hrpB_R	5' – CGAATGGCGGATCAGGCGCT target locus: RSp0873	This study
hrpG_F	5' – GCAGAACGTGGAATGTGTCC target locus: R.	This study

	solanacearump0852	
hrpG_R	5' – AGACTGAATGCCTCGGTACG target locus: RSp0852	This study
ripAA_F	5' – GGAATACAGCAACTGCGTGC target locus: RSc0608	This study
ripAA_R	5' – TTGTAGTTGCGGACCCTCAGtarget locus: RSc0608	This study
serC_F	5' – CGCGCAAATACGGTGAAGTG target locus: R. solanacearumc0903	This study
serC_R	5' – GTGCACAGATGCACGTAAGC target locus: RSc0903	This study
Actin_F	5' – TCAGCAACTGGGATGATATG target locus: BT013524	(Milling *et al.*, 2011)
Actin_R	5' – TTAGGGTTGAGAGGTGCTTC target locus: BT013524	(Milling *et al.*, 2011)

[a] Capitalized bp anneal to the target locus, non-capitalized bp anneal to other fragments in a Gibson assembly reaction

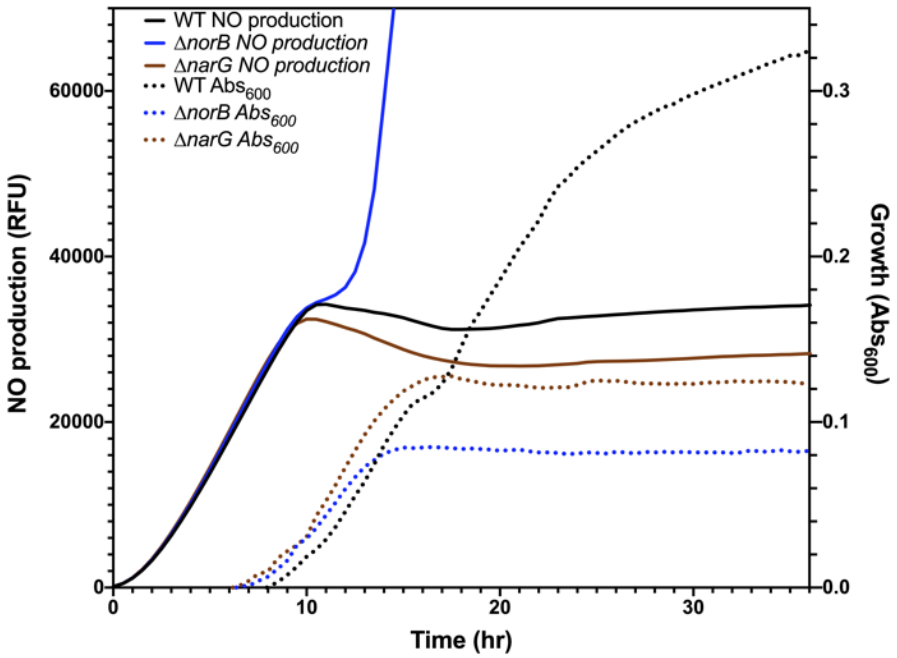

Supplementary Figure 1 Growth and NO levels of *R. solanacearum* strains under denitrifying conditions in culture. Cultures were started at a concentration of 10^6 CFU/mL in VDM containing the NO-detecting fluorescent dye DAF-FM DA at 10 μM. Cultures were incubated in in clear-bottomed, white-walled 96-well plates at 30C for 24 h at $[O_2]$ =0.1%. Culture growth (dotted lines) is shown as absorbance at 600 nm. NO concentration (solid lines) was measured as DAF-FM fluorescence at 495/515 nm. The *ΔnorB* mutant strain accumulates NO, which significantly impairs its growth.

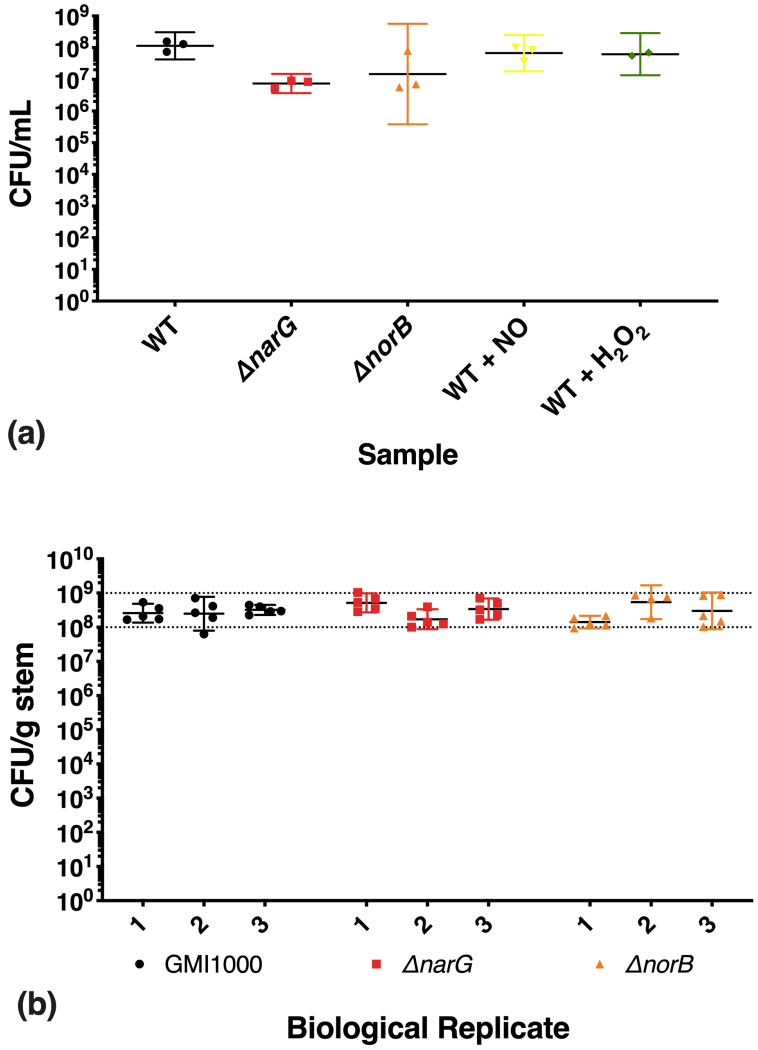

Supplementary Figure 2 In vitro cell densities and tomato stem colonization of samples used in RNA-seq. **(a)** Cell densities of culture samples as measured by dilution plating. One H_2O_2-treated plate was uncountable due to plate contamination. OD_{600} values of each culture were also collected and had comparable values. **(b)** Colonization of tomato plants used for transcriptome sequencing. Roughly 0.1 g of stem tissue was collected from directly below the sample used for sequencing. The tissue was ground and dilution plated to enumerate CFU/g stem.

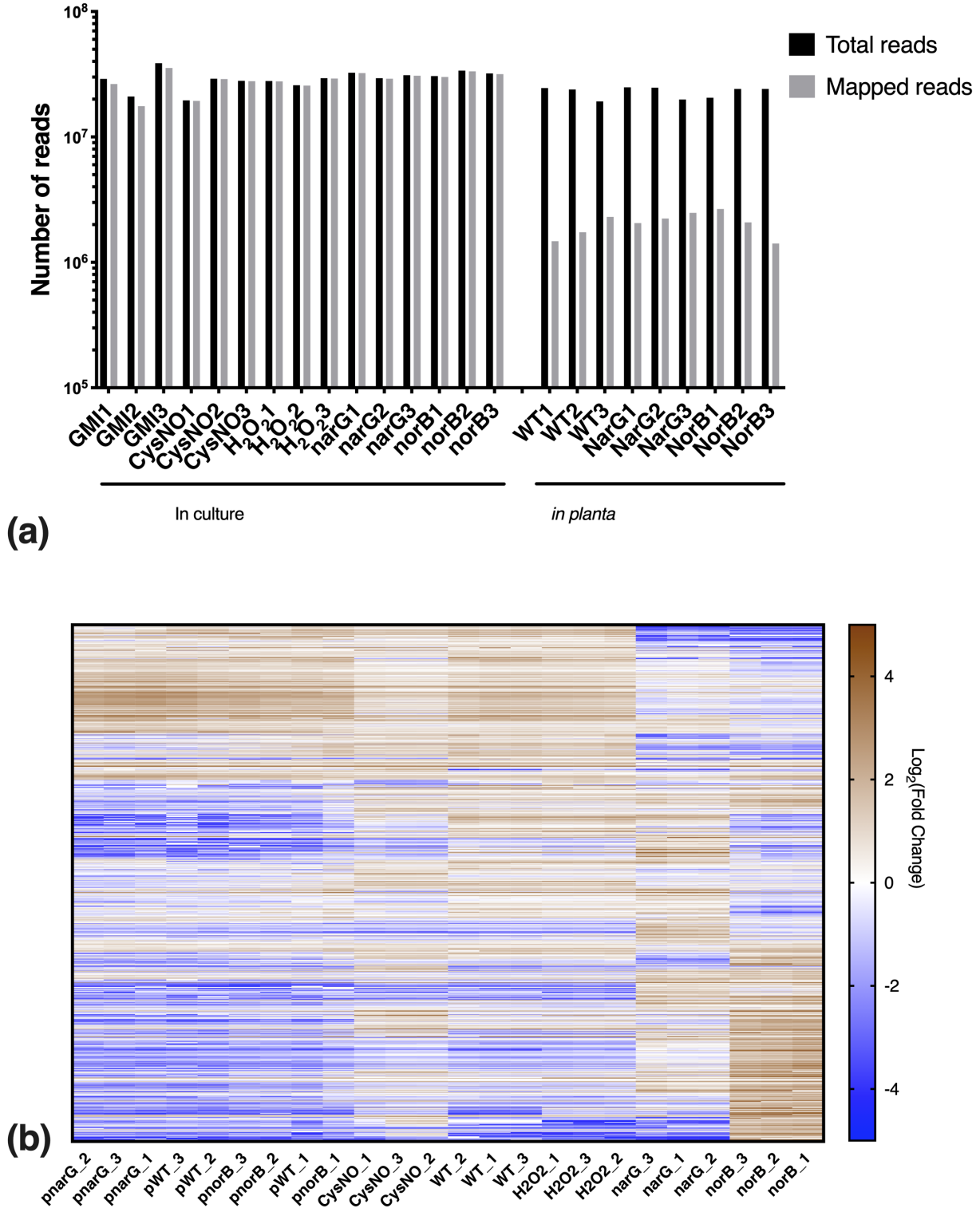

Supplementary Figure 3 (a) Total and mapped reads per RNA-seq sample. The *in planta* samples had lower percentage of mapped reads due to the presence of host RNA. **(b)** Hierarchical clustering and

788 expression heat map of the 1000 most variable genes in the dataset. Blue indicates higher expression
789 and brown indicates lower expression. All genes were normalized to the mean gene expression across all
790 conditions. Samples collected from *R. solanacearum* grown *in planta* are denoted with the prefix "p".
791 Heatmap created using iDEP.90 (Ge *et al.*, 2018).
792
793 **Supplementary Table 2** Complete list of gene expression and $\log_2$ fold change values for all conditions
794 included in this study. All fold-change numbers are compared to levels in untreated wild-type (WT) cells.
795 NO levels were modified genetically using mutants lacking *narG* (deleting this nitrate reductase reduces
796 endogenous NO) and *norB* (deleting this nitric oxide reductase increases endogenous NO). NO levels
797 were increased chemically by adding 1 mM CysNO. Cells treated with 100 μM hydrogen peroxide (H_2O_2)
798 were a non-NO control to identify general stress responses. *P*-values were calculated by DESeq were
799 adjusted to control for the false discovery rate (FDR) using the Benjamini-Hochberg approach.
800
801 **Supplementary Table 3** KEGG enrichment of genes altered in each condition. enrichment was
802 calculated using KOBAS v2.0 software. *P* values were calculated using a hypergeometric test and
803 adjusted using the Benjamini and Hochberg FDR correction method.
804
805 **Supplementary Table 4** Annotations, Log_2 fold change relative to wild-type and adjusted p-values for *R.*
806 *solanacearum* T3SS related genes in response to changes in NO concentration both *in planta* and in
807 culture (see Figure 3 for heatmap of these data). All fold-change numbers are compared to levels in
808 untreated wild-type (WT) cells. *in planta* samples are denoted by a 'p' in front of the treatment (e.g.
809 *pnorB*). Genes organized by their category, including structural genes, regulatory genes, chaperones, and
810 effectors. Effectors are subgrouped based on their known association with chaperones (Lonjon *et al.*,
811 2015).